


Article

Study on a Strong Polymer Gel by the Addition of Micron Graphite Oxide Powder and Its Plugging of Fracture

Bin Shi ^{1,2}, Guangming Zhang ^{1,*}, Lei Zhang ³, Chengjun Wang ⁴, Zhonghui Li ¹ and Fangping Chen ²

¹ Hubei Key Laboratory of Drilling and Production Engineering for Oil and Gas, School of Petroleum Engineering, Yangtze University, Wuhan 430100, China; stonersb2@163.com (B.S.); lizhonghui2024@163.com (Z.L.)

² Research Institute of Shaanxi Yanchang Petroleum (Group) Co., Ltd., Xi'an 710075, China; geda2024@163.com

³ Hubei Provincial Key Laboratory of Oil and Gas Exploration and Development Theory and Technology, Department of Petroleum Engineering, China University of Geosciences (Wuhan), Wuhan 430074, China; zhangshishishi.188@163.com

⁴ College of Chemistry and Chemical Engineering, Xi'an University of Petroleum, Xi'an 710065, China; 210104@xsyu.edu.cn

* Correspondence: zhanggm2024@163.com

Abstract: It is difficult to plug the fracture water channeling of a fractured low-permeability reservoir during water flooding by using the conventional acrylamide polymer gel due to its weak mechanical properties. For this problem, micron graphite powder is added to enhance the comprehensive properties of the acrylamide polymer gel, which can improve the plugging effect of fracture water channeling. The chemical principle of this process is that the hydroxyl and carboxyl groups of the layered micron graphite powder can undergo physicochemical interactions with the amide groups of the polyacrylamide molecule chain. As a rigid structure, the graphite powder can support the flexible skeleton of the original polyacrylamide molecule chain. Through the synergy of the rigid and flexible structures, the viscoelasticity, thermal stability, tensile performance, and plugging ability of the new-type gel can be significantly enhanced. Compared with a single acrylamide gel, after adding 3000 mg/L of micrometer-sized graphite powder, the elastic modulus, the viscous modulus, the phase transition temperature, the breakthrough pressure gradient, the elongation at break, and the tensile stress of the acrylamide gel are all greatly improved. After adding the graphite powder to the polyacrylamide gel, the fracture water channeling can be effectively plugged. The characteristics of the networked water flow channel are obvious during the injected water break through the gel in the fracture. The breakthrough pressure of water flooding is high. The experimental results are an attempt to develop a new gel material for the water plugging of a fractured low-permeability reservoir.

Keywords: enhanced oil recovery; water plugging; high strong polymer gel; graphite powder; breakthrough pressure



Citation: Shi, B.; Zhang, G.; Zhang, L.; Wang, C.; Li, Z.; Chen, F. Study on a Strong Polymer Gel by the Addition of Micron Graphite Oxide Powder and Its Plugging of Fracture. *Gels* **2024**, *10*, 304. <https://doi.org/10.3390/gels10050304>

Academic Editor: Michael Gradzielski

Received: 9 March 2024

Revised: 20 April 2024

Accepted: 23 April 2024

Published: 30 April 2024



Copyright: © 2024 by the authors. Licensee MDPI, Basel, Switzerland. This article is an open access article distributed under the terms and conditions of the Creative Commons Attribution (CC BY) license (<https://creativecommons.org/licenses/by/4.0/>).

1. Introduction

The Yanchang oilfield is a typical low-permeability oil reservoir with dense matrix pores and widespread natural micro-fractures. At the early stage of development, most oil wells undergo hydraulic fracturing to increase oil production, resulting in complex fracture networks within the reservoirs. However, as water injection operations deepen and injection-production schemes are adjusted, the injected water can flow through the fractures due to the high conductivity, leading to water breakthrough in the corresponding oil wells [1–5]. To address this issue, using gel to plug the fracture water channeling has been considered the most reliable measurement for the efficient development of such reservoirs [6–10]. Due to the strong and large-scale flow capacity of fractures, combined with the dense matrix and high injection water pressure, it requires a high strong gel with

good mechanical properties to effectively plug the fracture water channeling of a fractured low-permeability reservoir [11,12].

Presently, the underground cross-linked acrylamide polymer gel system is the most widely used water plugging agent, known for its mature technology, low cost, and safety [11,13–15]. This system (gelant) has a low initial viscosity under surface conditions, so it has a good injection performance. After entering the reservoir, the gelant undergoes a cross-linking reaction under the reservoir conditions to form a three-dimensional network structure so that it has a plugging ability [16,17]. After that, the gelant becomes a continuous and integral gel, which plays a role of water plugging. Nevertheless, the concentration of the acrylamide polymer gel system is generally low, and the mechanical strength of the formed gel is weak. The injected water easily breaks through the gel and forms a water channeling zone again in the fracture water channeling during the subsequent water flooding process. Although continuing to increase the concentration of the acrylamide polymer gel system can improve the mechanical strength of the formed gel, it leads to a significant increase in the initial viscosity of the system and the costs, which can cause difficulties in mixing during on-site liquid preparation, an inability to complete pumping operations, or pump operation damage [18–20]. Therefore, increasing the mechanical strength of acrylamide-based gels is one of the key factors in improving their effectiveness in plugging fracture water channeling.

Based on the size effect and surface/interface effects of micro-materials, the overall performance of composite gels can be significantly enhanced through the physical-chemical actions occurring during the process of adding micro-materials (such as coal fly ash, nano-SiO₂, clay mineral, etc.) to the gels [21–24]. However, there are some shortcomings for these gel systems. For example, the cost of nanomaterials is high. The performance of clay mineralized composite gel is not significantly improved. Therefore, it is necessary to develop new additives to improve the performance of polymer gel. In recent years, graphite materials have attracted much attention as a hot topic in the field of micro-materials [25–29]. The modified hydrophilic micron graphite powder has a layered structure with abundant hydroxyl and carboxyl functional groups on its surface, so it can be uniformly dispersed in water. An excellent material can be formed after the micron graphite powder is compounded with water-soluble polymers, and it is commercially available at a low price [30–35]. Therefore, it is technically and economically feasible to enhance the performance of polymer gels by adding micron graphite powder. In this study, by evaluating the influence of micron graphite powder on gel performance and characterizing the features of such composite gels for plugging the fracture water channeling, an attempt is made to develop a new technical system for water shut-off operations in fractured low-permeability reservoirs.

2. Results and Discussion

2.1. Effect of Micron Graphite Powder on the Structure of Polymer Gel

The infrared spectra of the two gel systems are shown in Figure 1. A comparison reveals that the micron graphite powder has a significant impact on the structure of acrylamide-based gels. In the spectrum of gel system 2, the characteristic absorption peaks of N–H groups are observed at 3400 cm⁻¹ and 3200 cm⁻¹. The stretching vibration peaks of carbonyl (C=O) groups and the bending vibration peak of N–H are observed at 1740 cm⁻¹ and 1660 cm⁻¹, respectively. The vibration peak at 1450 cm⁻¹ corresponds to methylene (CH₂) groups, and the stretching vibration peak of C–N is observed at 1365 cm⁻¹. Comparing the spectrum of gel system 2, there are shifted peaks at 1740 cm⁻¹ and 1660 cm⁻¹ and different peaks at 1450 cm⁻¹ and 1365 cm⁻¹. This shows that there is a physical and chemical reaction between the graphite powder and the polymer [36–39]. The principle of this process can be illustrated in Figure 2. It can be observed that the interaction between the abundant hydroxyl and carboxyl groups in the layered structure of micron graphite powder and the amide groups in the polyacrylamide chain occurs, so the gel has a stronger structure.

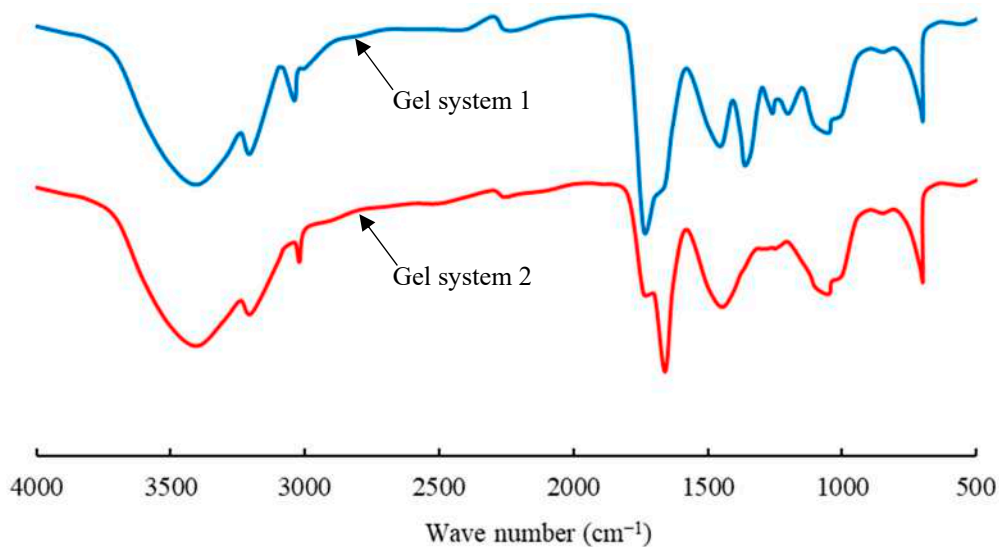


Figure 1. Infrared spectra of the two gels.

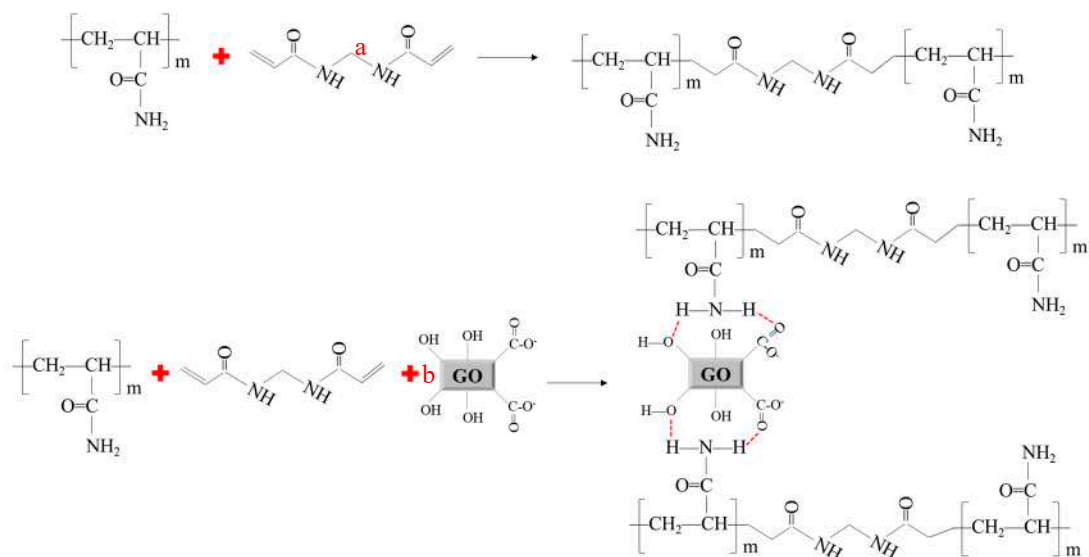


Figure 2. Mechanism of the cross-linking reaction of the two gels ((a): gel system 1; (b): gel system 2).

2.2. Effect of Micron Graphite Powder on the Viscoelasticity of Gels

The impact of the micron graphite powder on the viscosity of the gelant before and after gelation is shown in Figure 3. After the addition of graphene oxide, the initial viscosity of the gel solution remains almost unchanged, indicating that the addition of micron-sized graphite powder has little effect on the flow properties of the gelant solution. After gelation, the viscosity of the gel is increased from 13×10^4 mPa·s to 23×10^4 mPa·s, indicating that graphene oxide can significantly enhance the strength of the gel.

The impact of micron graphite powder on the viscoelasticity of the gel is shown in Figure 4. After the addition of micron graphite powder, both the elastic modulus and the viscous modulus of the gel are significantly increased, indicating a substantial improvement in the overall strength of the gel. For example, at 1 Hz, the elastic modulus is increased from 120 Pa to 400 Pa, and the viscous modulus is increased from 48.6 Pa to 268 Pa. Combined with the analysis of the infrared spectra, it can be inferred that the cross-linking density of the gel is enhanced due to interactions with the amide groups on the polyacrylamide chains. During the chemical reaction, the flexible acrylamide chains can form a three-dimensional network structure through copolymerization and cross-linking reactions. The added micron graphite powder can provide a rigid structure that can support the flexible framework of

the original gel acrylamide chains rather than just acting as a physical filler. The synergistic effect between the rigid and flexible structures can greatly enhance the viscoelasticity of the gel.

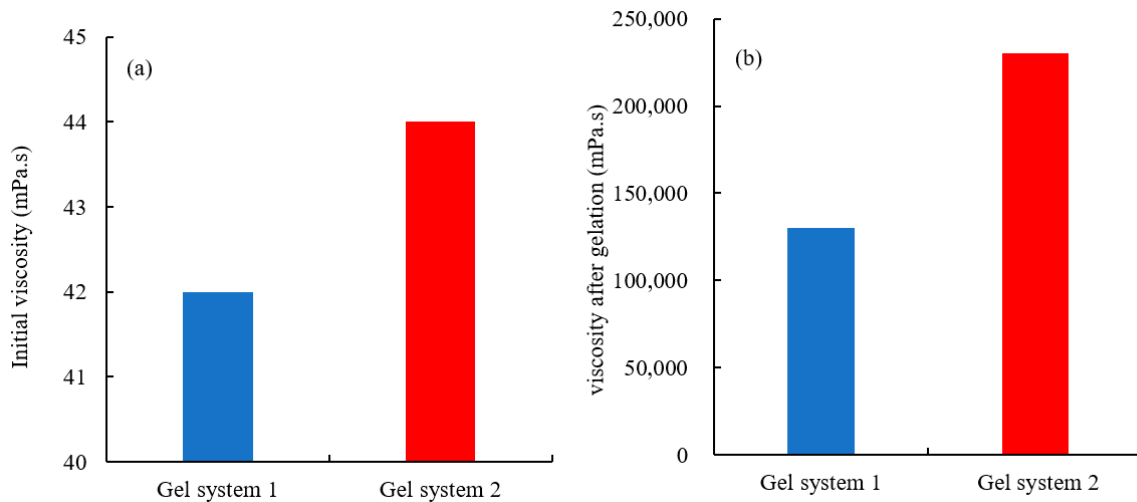


Figure 3. Viscosity of the two gels ((a): initial viscosity; (b): gel viscosity).

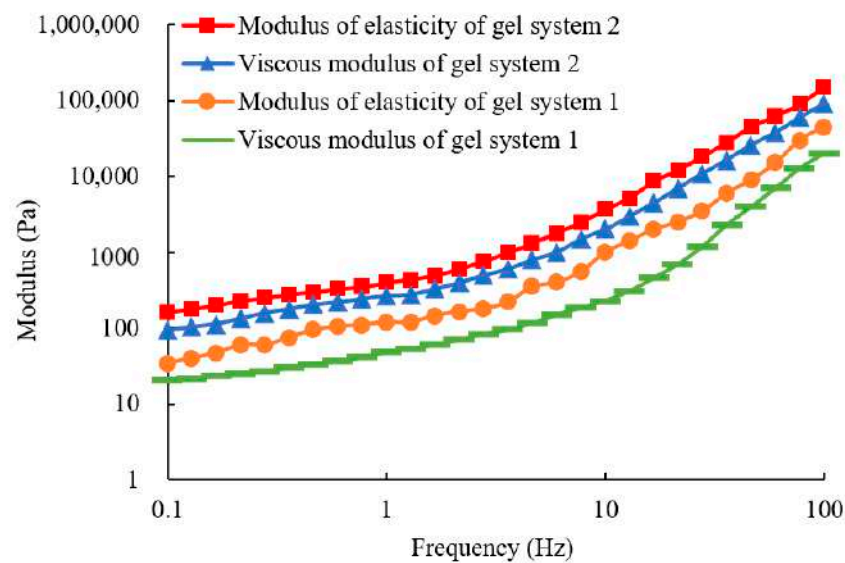


Figure 4. Viscoelasticity of the two types of gels.

2.3. Effect of Micron Graphite Powder on the Thermal Stability of Gels

The heat flow curves (DSC) of the two gel systems during the heating process are shown in Figure 5. In Figure 5, it can be observed that the phase transition temperature for gel system 1 is 167 °C, while it is 212 °C for gel system 2. A comparison reveals that the addition of micron graphite powder can significantly enhance the heat resistance of the gel. When the liquid water in the gel system transitions to gaseous water, the water molecules not only need to overcome the attractive forces between other water molecules but also break free from the constraints of the gel network structure. When the network structure of the gel remains stable, it is difficult for water molecules to escape due to capillary forces. As the temperature is increased, the network structure of the gel is disrupted, and water molecules can be rapidly detached from the gel, resulting in a significant increase in the heat flow rate. Comparing the temperature points corresponding to the rapid rise in the heat flow rate, gel system 2 reaches around 170 °C, while gel system 1 reaches around 120 °C, indicating that the addition of micron graphite powder can greatly improve the

heat resistance of the gel. The reason for this improvement lies in the fact that the added micron graphite powder participates in the gel formation process, leading to a denser three-dimensional network structure. Moreover, the micron graphite powder itself is an excellent heat-resistant material. Additionally, the surface effects and small size effects of the micron materials further enhance the firm binding of water molecules, thereby providing stronger heat resistance to gel system 2.

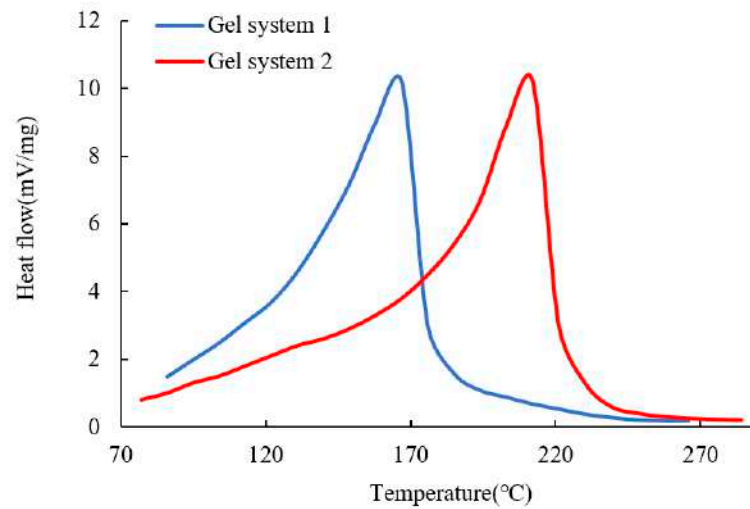


Figure 5. DSC curves of the two types of gels.

2.4. Effect of Micron Graphite Powder on the Tensile Properties of Gels

The stress–strain curves of the two gels are shown in Figure 6. In Figure 6, it can be observed that gel system 1 has an elongation of 700% and a tensile stress of 38 kPa. On the other hand, gel system 2 exhibits an elongation of 1100% and a tensile stress of 110 kPa. A comparison reveals that gel system 2 has a higher tensile strength. During the chemical crosslinking process of a single acrylamide-based gel, there are many disordered crosslinking points, and the distribution of gel crosslinking points is uneven. Regions with a lower crosslinking density become weak points in the gel structure and contribute to gel rupture under tension. However, during the chemical crosslinking process of a composite gel, the micron graphite powder acts as a partial crosslinking agent, leading to an overall increase in the crosslinking density of the gel and a significant improvement in its tensile properties [40].

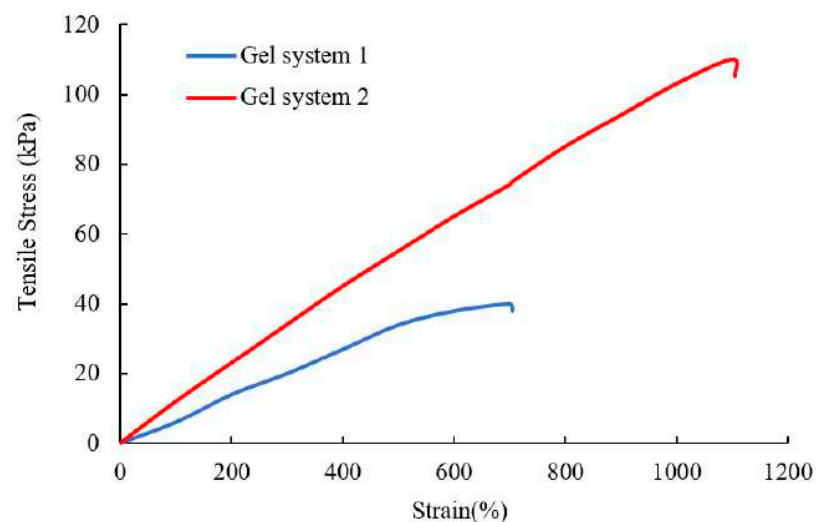


Figure 6. Stretching curves of the two types of gels.

2.5. Plugging Performance of the Gel System

The breakthrough pressures of the two gels in different fractures are shown in Figure 7. After the fracture water channelings are filled with the gel, the water flow pathway is plugged, and the water injection pressure gradient is increased and then decreased until it is stabilized. The peak value of the curve represents the breakthrough pressure gradient of the gel, which indicates the plugging strength of the gel in the fracture water channeling. The stable value of the curve represents the water flow resistance after the gel is broken by the injected water, which is the residual resistance gradient of the gel in the fracture water channeling. As the aperture of the fracture is increased, both the breakthrough pressure gradient and the residual resistance gradient are both decreased. When the apertures of the fractures are 0.13 mm and 0.24 mm, the breakthrough pressure gradients of gel system 2 are 440 kPa/m and 175 kPa/m, respectively, while the breakthrough pressure gradients of gel system 1 are 255 kPa/m and 120 kPa/m, respectively. The experimental results indicate that the addition of micron graphite powder can significantly enhance the plugging strength of the gel. This is due to the fact that the micron graphite powder strengthens the gel's viscoelasticity, tensile strength, and other properties.

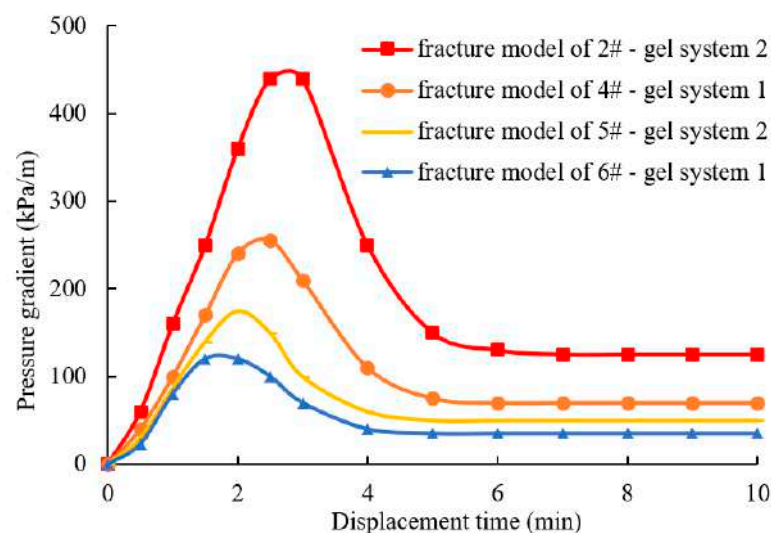


Figure 7. Breakthrough pressure gradient of the gel in fractures with different openings.

During the subsequent water flooding process, the changes in the water injection pressure gradient are due to the breakthrough of the injected water through the gel in the fractures. The breakthrough behavior is shown in Figure 8 (the green fluid is the stained water, and the transparent part is the gel). From Figure 8, it can be observed that when the apertures of fractures are different, the penetration of injected water through the gel takes on different forms. In a smaller aperture of a fracture, such as fracture model #2, the injected water breaks through the gel and forms a mesh-like water flow channel. However, in a larger aperture of a fracture, such as fracture model #5, a strip-like water flow channel is formed. By comparing the plugging characteristics of the two in different fractures, it can be concluded that the stronger the gel, the more pronounced the mesh-like water flow channel characteristic, and the weaker the gel, the more pronounced the strip-like water flow channel characteristic. The smaller aperture of the fracture corresponds to the stronger gel, larger water injection pressure gradient, and higher energy required for water to penetrate through the gel, resulting in temporary pressure accumulation in multiple locations of the fracture, forming a mesh-like fracture. Larger fracture apertures correspond to the weaker gel and lower plugging strength, making it easier for the injected water to penetrate the weakest part of the cross-linking gel, thus forming a strip-like rupture.

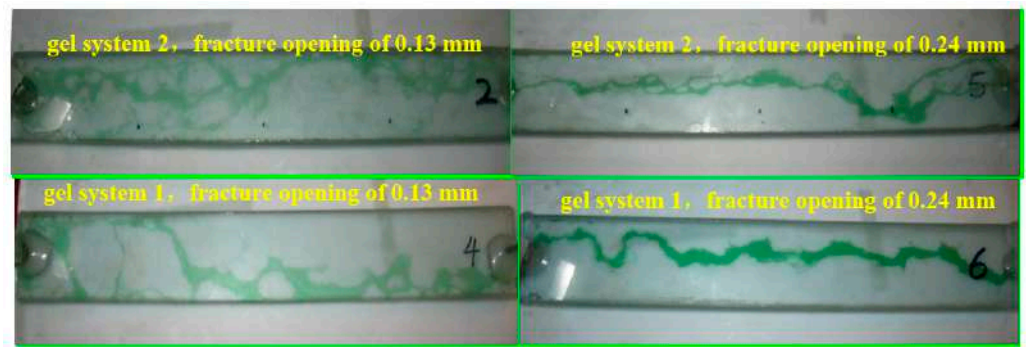


Figure 8. Morphology of water injection penetrating into the gel under different apertures of fracture (the green fluid is the stained water, and the transparent part is the gel).

After processing the data, it is found that the breakthrough pressure gradient is inversely proportional to the square of the aperture of the fracture, as shown in Figure 9. The aperture of the fracture has a significant impact on the plugging behavior of the gel in the fractures. Based on the results in Figure 9, the breakthrough pressure gradient of the gel can be obtained according to the size of the aperture of the fracture.

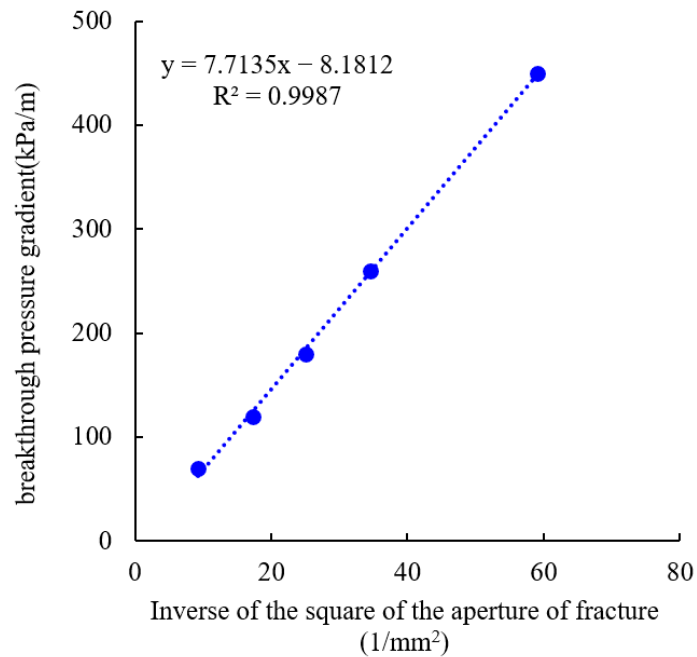


Figure 9. Relationship between the breakthrough pressure gradient and the inverse of the square of the aperture of the fracture.

2.6. The Plugging Ability of the Graphene Oxide Gel System to Enhance Oil Recovery

The change in the oil recovery and water cut during plugging by using the gel in the fractured core is shown in Figure 10. Owing to the strong heterogeneity of the fracture, the water cut of the primary water flooding is almost 100%, and the oil recovery is almost minimal. After the fracture is plugged, the oil in the matrix can be displaced by the water flow. During the subsequent waterflooding, when the water cut is gradually increased to 98% again, the oil recovery is increased by 28%.

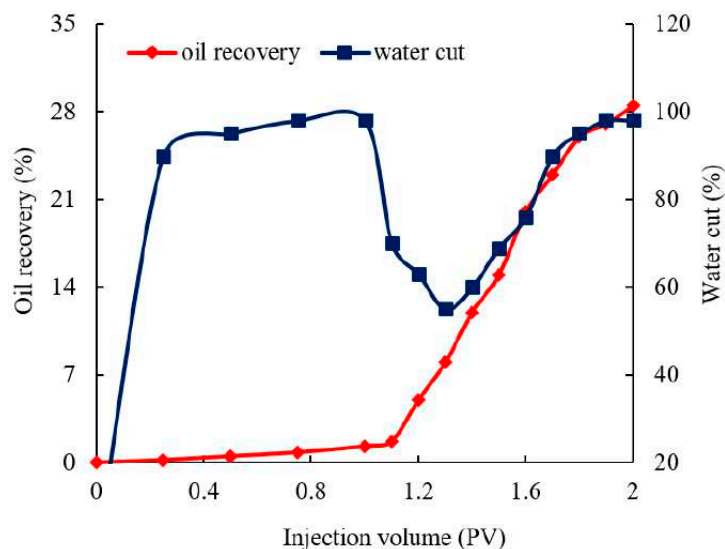


Figure 10. Changes in the oil recovery and water cut of the fractured core during water flooding before and after plugging.

3. Conclusions

(1) Adding the micron graphite powder to polyacrylamide gel can significantly enhance the gel's viscoelasticity, thermal stability, tensile strength, and plugging ability. The improvement is attributed to the interaction of the hydroxyl and carboxyl groups on the micron graphite powder layers and the amide groups on the polyacrylamide molecular chains. The micron graphite powder acts as a crosslinking agent, not only physically filling the gaps but also providing rigid support to the flexible main chains, thereby enhancing the comprehensive properties of the gel. Adding 3000 mg/L of oxidized graphene can greatly improve the comprehensive performance of the gel, increasing the elastic modulus from 120 Pa to 400 Pa and the viscous modulus from 50 Pa to 280 Pa under a frequency of 1 Hz. The thermal transition temperature can also be increased from 167 °C to 212 °C, and the tensile stress can be increased from 40 kPa to 110 kPa.

(2) During the process of plugging a fracture, when the gel is stronger, a network-like water flow channel is formed, while a strip-like water flow channel is formed when the gel is weaker. By using the micron graphite powder composite gel for plugging the fracture, the characteristics of a network-like water flow channel become evident, indicating a high plugging strength. In field construction, the stronger composite gel plugging agents can be used as segment plugs, resulting in lower implementation costs and higher economic feasibility. During the process of plugging a fracture, the breakthrough pressure gradient is decreased with the increase in the aperture of the fracture. The apertures of the fracture are 0.13 mm, 0.17 mm, 0.2 mm, 0.24 mm, and 0.33 mm, corresponding to breakthrough pressure gradients of 440 kPa/m, 250 kPa/m, 175 kPa/m, 120 kPa/m, and 70 kPa/m, respectively. The breakthrough pressure gradient is inversely proportional to the square of the aperture of the fracture. Different apertures of the fracture result in different water infiltration patterns through the gel. In small fractures, a network-like water channel is formed, while in larger fractures, a strip-like water channel is formed. The use of micron graphite powder in combination with traditional acrylamide-based gels can provide a strong material foundation for plugging the fractured low-permeability reservoir.

4. Materials and Methods

4.1. Materials

The reservoir water was simulated by preparing a solution of 10 g/L NaCl in tap water. All the solutions in the experiment were prepared by using simulated reservoir water. The micron graphite powder with a layered structure (containing a large number of hydroxyl and carboxyl groups on its surface) is a commercially available product

provided by Nanjing Xianfeng Nano-Material Technology Co., Ltd, Nanjing, China. The content of oxygen-containing groups on the used graphite is 0.015 mmol/g. The particle size distribution of the graphite powder is 0.5–5 μm , and it has a low cost, making it suitable for industrial applications. Acrylamide (AM), N,N'-Methylenebisacrylamide, and potassium persulfate are all of analytical purity and were purchased from China National Pharmaceutical Group Chemical Reagent Co., Ltd, Beijing, China.

4.2. Instruments and Apparatus

A Brookfield viscometer, Brookfield company (Middleboro, MA, USA); RS-600HAAKE rheometer, Haake company (Karlsruhe, Germany); Nicolet 6700 Fourier Transform Infrared Spectrometer (FTIR), Thermo Fisher company (Waltham, MA, USA); DSC823 Differential Scanning Calorimeter, Mettler Toledo company (Zurich, Switzerland); and Anton-Paar Dynamic Mechanical Analyzer, Anton-Paar company (Graz, Austria), were used. A conventional physical simulation displacement experimental apparatus, Hai'an Petroleum Research Instruments Co., Ltd. (Hai'an, China), was used. For the plugging experiments, a visually observable fracture model was created to simulate reservoir fractures. This fracture model was formed by bonding two pieces of frosted glass along the sides by using epoxy resin adhesive. The aperture of the fracture was controlled by filling rubber bands with different sizes on the fracture surface. The parameters of the fractures used in the experiment are shown in Table 1. The temperature of the displacement experiment is 45 $^{\circ}\text{C}$, and the injection rate of the fluid is 0.5 mL/min. The inlet of the fracture model is connected to a pressure sensor, and the inlet pressure is automatically recorded by the computer. The outlet of the fracture model is connected to the atmosphere. The pressure difference (ΔP) at both ends of the fracture model is numerically equal to the inlet pressure.

Table 1. Parameters of fracture models.

| No. | Fracture Length (cm) | Fracture Width (cm) | Diameter of Rubber Bands (Mesh Number/mm) | Fracture Aperture (mm) |
|-----|----------------------|---------------------|---|------------------------|
| #2 | 25 | 2.5 | 180/0.08 | 0.13 |
| #4 | | | 180/0.08 | 0.13 |
| #5 | | | 70/0.2 | 0.24 |
| #6 | | | 70/0.2 | 0.24 |

4.3. Experimental Methods

4.3.1. Static Experiments

The composition of gel system 1 is 40,000 mg/L of acrylamide monomer, 2000 mg/L of N, N'-Methylenebisacrylamide (crosslinker), and 600 mg/L of potassium persulfate (initiator). The composition of gel system 2 is 3000 mg/L of micron graphite powder, 40,000 mg/L of acrylamide monomer, 2000 mg/L of N, N'-Methylenebisacrylamide (crosslinker), and 600 mg/L of potassium persulfate (initiator).

The gelation experiment is conducted at a temperature of 45 $^{\circ}\text{C}$. The viscosity of the gel system is measured by using a viscometer at a shear rate of 7.34 s^{-1} . The viscoelasticity of the gel system is measured by using a rheometer at different frequencies. The structure of the gel system is determined by using FTIR spectroscopy. The thermal stability of the gel system is determined by using a differential scanning calorimeter (DSC) at a heating rate of 3 $^{\circ}\text{C}/\text{min}$. The temperature range for heating is from 50 to 800 $^{\circ}\text{C}$, and nitrogen gas is used as the protective atmosphere. The mechanical properties of the gel system are determined by using a dynamic mechanical analyzer. Based on the results of the static tests of the two gel systems, the effect of micron graphite powder on the performance of acrylamide-based gels can be investigated.

4.3.2. Dynamic Experiments

The simulation experiment device for displacement is shown in Figure 11. One is the visual fracture displacement experiment. The other is the fractured core displacement experiment. During the visual fracture displacement experiment, the 1PV of gel system 1 is injected into the fracture models of #4 and #6, respectively. The 1PV of gel system 2 is injected into the fracture models of #2 and #5, respectively. Thus, after gelation, the breakthrough pressure is measured. The method of measurement is as follows. After the plugging agent in the fracture is fully gelled, the subsequent water flooding is conducted and the simulated formation water is injected into the fractures until the flow rate at the outlet is suddenly increased and the inlet pressure of the fracture is decreased. The inflection point on the injection pressure curve represents the breakthrough pressure. The experimental temperature is 45 °C and the injection rate is 0.5 mL/min. A pressure sensor is connected to the inlet of the fracture, and the inlet pressure is automatically recorded by the computer. The outlet of the fracture is exposed to atmospheric pressure, and the pressure difference ΔP between the two ends is numerically equal to the inlet pressure.

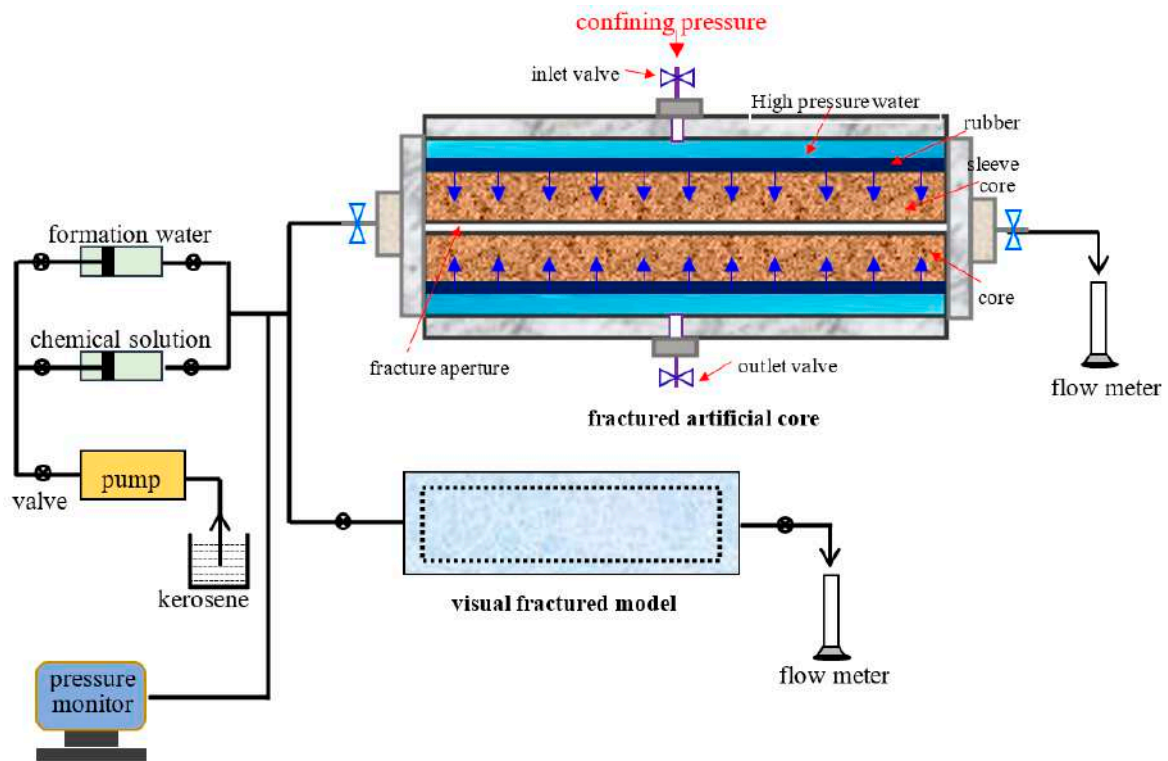


Figure 11. Simulation experiment device for core displacement and visual fractured model displacement [1].

During the fractured core displacement experiment, a natural outcrop core with the size of 45 mm width \times 45 mm height \times 300 mm length and a water permeability of $1 \times 10^{-3} \mu\text{m}^2$ is used to be processed into a fractured core. The aperture of the fracture is 0.24 mm. After the fractured core is saturated oil, it is displaced by the simulated water at an injection rate of 0.5 mL/min until the water cut at the outlet is up to 98%. Thus, 1 FPV of the plugging agent of the micron graphite powder–polymer composite gel is injected into the fractured core. After gelation, the subsequent water flooding is carried out again until the water cut of the effluent is 98%. Thus, the changes in the oil recovery before and after plugging can be obtained.

Author Contributions: Conceptualization, B.S. and L.Z.; Methodology, B.S. and L.Z.; Software, B.S. and L.Z.; Validation, B.S. and L.Z.; Writing—review & editing, Z.L. and F.C.; Supervision, G.Z. and C.W.; Project administration, G.Z. and C.W. All authors have read and agreed to the published version of the manuscript.

Funding: This study was supported by the National Natural Science Foundation of China (No. 52204054) and the Innovation Capacity Support Program of Shaanxi (Program No. 2023-CX-TD-31).

Data Availability Statement: The original contributions presented in the study are included in the article, further inquiries can be directed to the corresponding authors.

Conflicts of Interest: B.H. and F.C. were employed by the Research Institute of Shaanxi Yanchang Petroleum (Group) Co., Ltd. The remaining authors declare that the research was conducted in the absence of any commercial or financial relationships that could be construed as a potential conflict of interest.

References

- Zhang, L.; Khan, N.; Pu, C. A new method of plugging the fracture to enhance oil production for fractured oil reservoir by using gel particles and HPAM/Cr³⁺ system. *Polymers* **2019**, *11*, 446. [[CrossRef](#)] [[PubMed](#)]
- Chen, S.; Hui, F.; Wei, W.; Zhang, T.; Wu, X.; Nie, J. Study on water plugging and fracturing technology for water flooded oil wells in low-permeability reservoir. *Fresenius Environ. Bull.* **2022**, *31*, 6221–6229.
- Liu, K.; Zhu, W.; Pan, B. Laboratory evaluation on oil-soluble resin as selective water shut-off agent in water control fracturing for low-permeability hydrocarbon reservoirs with bottom aquifer. *Geoenergy Sci. Eng.* **2023**, *225*, 2949–8910. [[CrossRef](#)]
- Yang, Y.; Liao, G.; Xiong, W.; Shen, R.; Zhang, J.; Wang, S.; Zhang, J.; Tan, L.; Shao, G. Physical and numerical simulation of inter-fracture flooding in heterogeneous tight oil reservoirs. *Energy Rep.* **2022**, *8*, 12970–12978. [[CrossRef](#)]
- Chen, X.; Zhao, L.; Liu, P.; Du, J.; Bai, Z.; Liu, J.; Zhang, N.; Luo, Z.; Xu, K.; Li, N. Laboratory study and field verification of a thermo-responsive water shutoff agent. *J. Pet. Sci. Eng.* **2021**, *201*, 0920–4105. [[CrossRef](#)]
- Li, X.; Su, L.; Fu, M.; Li, Q.; Wang, Y. Study on plugging mechanism of gel plugging agent in fractured carbonate oil reservoirs. *Chem. Technol. Fuels Oils* **2023**, *59*, 507–516. [[CrossRef](#)]
- Fan, X.; Zhao, P.; Zhang, Q.; Zhang, T.; Zhu, K.; Zhou, C. A polymer plugging gel for the fractured strata and its application. *Materials* **2018**, *11*, 856. [[CrossRef](#)] [[PubMed](#)]
- Wang, J.; Wang, R.; Liu, P.; Xu, H. Gel-Forming and Plugging Performance Evaluation of Emulsion Polymer Crosslinking System in Fractured Carbonate Rock. *Processes* **2022**, *10*, 1550. [[CrossRef](#)]
- Luo, Z.; Zhao, L.; Liu, P.; Wang, Z. Integrated technology of water plugging and acidizing of hydrofractured oil wells. *Chem. Technol. Fuels Oils* **2015**, *51*, 190–198. [[CrossRef](#)]
- Kang, W.; Wang, J.; Ye, Z.; Gu, G.; Li, W.; Yang, H.; Li, Z.; Xu, H.; Lv, Z.; Sarsenbekuly, B. Study on preparation and plugging effect of sawdust gel particle in fractured reservoir. *J. Pet. Sci. Eng.* **2022**, *212*, 110358. [[CrossRef](#)]
- Wu, Q.; Ge, J.; Zhang, G.; Guo, G.; Zhao, Q. Water plugging simulation experiment of high strength water plugging agent crack thin tube model. *Acta Pet. Sin.* **2019**, *40*, 1368–1375.
- Li, Z.; Li, X.; Du, K.; Liu, H. Development of a new high-temperature and high-strength polymer gel for plugging fractured reservoirs. *Upstream Oil Gas Technol.* **2020**, *5*, 100014. [[CrossRef](#)]
- Zhang, L.; Pu, C.; Cui, S.; Nasir, K.; Liu, Y. Experimental study on a new type of water shutoff agent used in fractured low permeability reservoir. *J. Energy Resour. Technol. Trans. ASME* **2017**, *139*, 012907. [[CrossRef](#)]
- Liu, R.; Yu, P. Research progress of high temperature resistant polymer gel plugging agent. *Appl. Chem. Ind.* **2021**, *50*, 736–740.
- Seidy Esfahlan, M.; Khodapanah, E.; Tabatabaei-Nezhad, S.A.; Salami-Kalajahi, M. Fabrication, optimization and characterization of preformed-particle-gel containing nanogel particles for conformance control in oil reservoirs. *Polym. Bull.* **2022**, *79*, 7137–7159. [[CrossRef](#)]
- Bai, B.J.; Leng, J.Q.; Wei, M.Z. A comprehensive review of in-situ polymer gel simulation for conformance control. *Pet. Sci.* **2022**, *19*, 189–202. [[CrossRef](#)]
- Zhao, H.; Zhao, P.; Bai, B.; Xiao, L.; Liu, X. Using associated polymer gels to control conformance for high temperature and high salinity reservoirs. *J. Can. Pet. Technol.* **2006**, *45*, 49–54. [[CrossRef](#)]
- Ghriga, M.A.; Grassl, B.; Gareche, M.; Khodja, M.; Lebouachera, S.E.; Andreu, N.; Drouiche, N. Review of recent advances in polyethylenimine crosslinked polymer gels used for conformance control applications. *Polym. Bull.* **2019**, *76*, 6001–6029. [[CrossRef](#)]
- Kang, W.L.; Kang, X.; Lashari, Z.A.; Li, Z.; Zhou, B.B.; Yang, H.B.; Sarsenbekuly, B.; Aidarova, S. Progress of polymer gels for conformance control in oilfield. *Adv. Colloid. Interface Sci.* **2021**, *289*, 102363. [[CrossRef](#)]
- Zhang, H.W.; Yang, H.B.; Sarsenbekuly, B.; Zhang, M.; Jiang, H.Z.; Kang, W.L.; Aidarova, S. The advances of organic chromium based polymer gels and their application in improved oil recovery. *Adv. Colloid. Interface Sci.* **2020**, *282*, 102214. [[CrossRef](#)]
- Saghafi, H.; Naderifar, A.; Gerami, S.; Emadi, M. Improvement in thermo-chemical stability of nanocomposite preformed particle gels for conformance control in harsh oil reservoir conditions. *Can. J. Chem. Eng.* **2016**, *94*, 1880–1890. [[CrossRef](#)]

22. Durán-Valencia, C.; Bai, B.; Reyes, H.; Fajardo-López, R.; Barragán-Aroche, F.; López-Ramírez, S. Development of enhanced nanocomposite preformed particle gels for conformance control in high-temperature and high-salinity oil reservoirs. *Polym. J.* **2014**, *46*, 277–284. [[CrossRef](#)]
23. Adewunmi, A.A.; Ismail, S.; Sultan, A.S. Investigation into the viscoelastic response at various gelation performance, thermal stability and swelling kinetics of fly ash reinforced polymer gels for water control in mature oilfields. *Asia Pac. J. Chem. Eng.* **2017**, *12*, 13–24. [[CrossRef](#)]
24. Aguiar, K.; Pereira, K.; Mendes, M.; Pedroni, L.; Oliveira, P.; Mansur, C. Study of the modification of bentonite for the formation of nanocomposite hydrogels with potential applicability in conformance control. *J. Pet. Sci. Eng.* **2020**, *195*, 107600. [[CrossRef](#)]
25. Wang, C.; Zhang, L.; Ju, G.; Sun, Q. Development and performance evaluation of a high-temperature profile control system. *ACS Omega* **2020**, *5*, 17828–17838. [[CrossRef](#)]
26. Kruglenko, E.; Korczak, I.; Litniewski, J.; Gambin, B. Ultrasound thermal effect enriched by adding of micro and nano particles to the agar-gel tissue mimicking materials. In Proceedings of the 2018 Joint Conference-Acoustics, Acoustics 2018, Ustka, Poland, 11–14 September 2018; pp. 158–163. [[CrossRef](#)]
27. Lu, A.; Liu, Q.; Zhao, G.; Xu, B.; Li, J.; Ni, M.; Dai, C. Preparation and enhancement mechanisms of a novel modified nanographite hybrid polymer gel for profile control in deep reservoirs. *Colloids Surf. A Physicochem. Eng. Asp.* **2023**, *681*, 132774. [[CrossRef](#)]
28. Chen, Y.; Liu, Y.; Zhao, H.; Teng, C.; Chen, S. Micro-characterization and mechanical properties of pseudo-boehmite stone-coated graphene oxide/epoxy resin-cyanate composites. *Acta Mater. Compos. Sin.* **2021**, *38*, 2855–2861.
29. Cote, L.; Kim, J.; Tung, V.; Luo, J.; Kim, F.; Huang, J. Graphene oxide as surfactant sheets. *Pure Appl. Chem.* **2011**, *83*, 95–110. [[CrossRef](#)]
30. Jiang, G.; Wang, G.; Hu, Q. Experimental study on enhancement of emulsifying acid energy by graphene oxide nanoparticles. *Appl. Chem. Ind.* **2020**, *49*, 3008–3010+3015.
31. Li, P.; Zhang, C.; Dai, X.; Sui, Y. Research progress of graphene oxide/polymer composite hydrogels. *Chem. J. Chin. Univ.* **2021**, *42*, 1694–1703.
32. Cho, H.; Yang, H.; Dong, J.; Kim, B.J. Surface engineering of graphene quantum dots and their applications as efficient surfactants. *ACS Appl. Mater. Interfaces* **2015**, *7*, 8615–8621. [[CrossRef](#)] [[PubMed](#)]
33. Chen, Y.; Li, X.; Zheng, S.; Tian, Y.; Zhu, R.; Feng, X.; Liu, C.; Zhang, Y. Preparation and properties of modified graphene oxide/polyacrylamide composite nanoparticle gel system. *J. Appl. Polym. Sci.* **2022**, *139*, 42. [[CrossRef](#)]
34. Qin, D.; Gao, W.; Zhang, S.; Cui, X.; Chen, H.; Yang, P.; Zheng, X. In situ composite of graphene oxide in polyacrylamide to enhance strength of hydrogel with polyethyleneimine as crosslinker. *Geoenergy Sci. Eng.* **2023**, *231*, 212304. [[CrossRef](#)]
35. Cao, J.; Xu, G.; Wang, X.; Liu, K.; Zhang, J.; Wang, H.; Wang, X.; Wu, Z. Engineering network entanglement of functionalized graphene oxide/poly(acrylamide) nanocomposites for enhanced oil recovery. *J. Mol. Liq.* **2022**, *360*, 119501. [[CrossRef](#)]
36. Peng, S.S.; Zhang, D.Q.; Huang, H.H.; Jin, Z.J.; Peng, X.H. Ionic polyacrylamide hydrogel improved by graphene oxide for efficient adsorption of methylene blue. *Res. Chem. Intermed.* **2019**, *45*, 1545–1563. [[CrossRef](#)]
37. Xu, Y.C.; Little, M.W.; Rousell, D.J.; Laboy, J.L.; Murray, K.K. Direct from polyacrylamide gel infrared laser desorption/ionization. *Anal. Chem.* **2004**, *76*, 1078–1082. [[CrossRef](#)]
38. Cheng, W.M.; Hu, X.M.; Xie, J.; Zhao, Y.Y. An intelligent gel designed to control the spontaneous combustion of coal: Fire prevention and extinguishing properties. *Fuel* **2017**, *210*, 826–835. [[CrossRef](#)]
39. GhavamiNejad, A.; Hashmi, S.; Joh, H.I.; Lee, S.; Lee, Y.S.; Vatankeh-Varnoosfaderani, M.; Stadler, F.J. Network formation in graphene oxide composites with surface grafted PNIPAM chains in aqueous solution characterized by rheological experiments. *Phys. Chem. Chem. Phys.* **2014**, *16*, 8675–8685. [[CrossRef](#)]
40. Chen, L.; Wang, J.; Yu, L.; Zhang, Q.; Fu, M.; Zhao, Z.; Zuo, J. Experimental investigation on the nanosilica reinforcing polyacrylamide/polyethyleneimine hydrogel for water shutoff treatment. *Energy Fuels* **2018**, *32*, 6650–6656. [[CrossRef](#)]

Disclaimer/Publisher’s Note: The statements, opinions and data contained in all publications are solely those of the individual author(s) and contributor(s) and not of MDPI and/or the editor(s). MDPI and/or the editor(s) disclaim responsibility for any injury to people or property resulting from any ideas, methods, instructions or products referred to in the content.